sustainability

MDPI

Article

Compensation Admittance Load Flow: A Computational Tool for the Sustainability of the Electrical Grid

Benedetto-Giuseppe Risi [1,2], Francesco Riganti-Fulginei [1,*], Antonino Laudani [1] and Michele Quercio [1]

[1] Department of Industrial, Electronic and Mechanical Engineering, University of Roma Tre, Via Vito Volterra 62, 00146 Rome, Italy; benedettogiuseppe.risi@uniroma3.it (B.-G.R.); alaudani@uniroma3.it (A.L.); michele.quercio@uniroma3.it (M.Q.)
[2] E-Grids SPA, Enel Group, Via Mantova 24, 000198 Rome, Italy
* Correspondence: francesco.rigantifulginei@uniroma3.it

Abstract: Compensation Admittance Load Flow (CALF) is a power flow analysis method that was developed to enhance the sustainability of the power grid. This method has been widely used in power system planning and operation, as it provides an accurate representation of the power system and its behavior under different operating conditions. By providing a more accurate representation of the power system, it can help identify potential problems and improve the overall performance of the grid. This paper proposes a new approach to the load flow (LF) problem by introducing a linear and iterative method of solving LF equations. The aim is to obtain fast results for calculating nodal voltages while maintaining high accuracy. The proposed CALF method is fast and accurate and is suitable for the iterative calculations required by large energy utilities to solve the problem of quantifying the maximum grid acceptance capacity of new energy from renewable sources and new loads, known as hosting capacity (HC) and load capacity (LC), respectively. Speed and accuracy are achieved through a properly designed linearization of the optimization problem, which introduces the concept of compensation admittance at the node. The proposed method was validated by comparing the results obtained with those coming from state-of-the-art methods.

Keywords: RESs (renewable energy systems); GS (Gauss–Seidel); NR (Newton–Raphson); LF (load flow); KPIs (key performance indicators)

Citation: Risi, B.-G.; Riganti-Fulginei, F.; Laudani, A.; Quercio, M. Compensation Admittance Load Flow: A Computational Tool for the Sustainability of the Electrical Grid. *Sustainability* **2023**, *15*, 14427. https://doi.org/10.3390/su151914427

Academic Editors: Dmitry Baimel, Ilan Aharon and Luis Hernández-Callejo

Received: 25 July 2023
Revised: 16 September 2023
Accepted: 25 September 2023
Published: 2 October 2023

1. Introduction

In recent years, the landscape of electricity generation has undergone a transformative shift from centralized production to a distributed generation (DG) model, necessitating substantial adaptations within the electricity grid framework. The conventional architecture of distribution grids, originally designed for passive operations with radial topologies and unidirectional power flows towards high-to-low voltage (HV to LV) substations, has proven inadequate for accommodating the significant integration of distributed generation [1,2]. As the demand for electricity escalates and distributed renewable sources gain widespread adoption [3], the need to modernize grid infrastructure and implement advanced monitoring and regulation technologies becomes imperative [4,5].

Within this evolving energy paradigm, the accurate assessment of load flow and optimal power distribution [6,7] emerges as a critical factor in effectively managing and forecasting the state and trajectory of the electrical grid. This assessment not only offers insights into optimizing resource allocation for harnessing existing grid capacity, but also aids in the seamless integration of new renewable energy systems (RESs) [8] and the accommodation of emerging loads [9–12]. Given that resolving the load flow problem serves as a cornerstone in optimizing power grid operations, the availability of efficient computational tools [13,14] is of paramount importance.

Against this backdrop, this paper introduces a novel methodology known as Compensation Admittance Load Flow (CALF), a hybrid approach that leverages the strengths of

both the Newton–Raphson (NR) [15] and Gauss–Seidel (GS) [15] methods under certain grid conditions. By explicating the methodological foundations, practical applications, and computational intricacies of CALF, this study aims to offer a comprehensive overview of the Compensation Admittance Load Flow approach.

Furthermore, this paper culminates in a rigorous series of tests that not only compare the Compensation Admittance Load Flow (CALF) method with established techniques like NR and GS, but also subject the method to rigorous scrutiny, encompassing performance and robustness [1,15,16]. Through the ensuing presentation, analysis, and discussion of these tests, the strengths, limitations, and unique attributes of the proposed CALF method are highlighted. By addressing the advantages and disadvantages of existing load flow methods, this paper effectively positions CALF within the broader context of power systems analysis, thereby providing a holistic evaluation of its contributions.

The distinctiveness of this work lies in the development of the Compensation Admittance Load Flow (CALF) method and its comparison with traditional Newton–Raphson and Gauss–Seidel methods. In a field as vital as electrical networks, where efficient load flow analysis is a cornerstone, the introduction of a linear and iterative approach like CALF represents a noteworthy advancement. By fusing the positive attributes of traditional methods with a particular focus on medium- and low-voltage scenarios, this method showcases the potential for rapid and accurate calculations, cost-effective simulations, and the ability to address intricate scenarios. Furthermore, its linear nature offers implementation advantages, particularly valuable for companies mandated to deploy complex algorithms for relatively straightforward scenarios.

Through an exhaustive comparison of simulation results across networks of varying sizes, this study validates the novel CALF methodology. By providing a meticulous analysis and introducing a new method, this work contributes significantly to the existing load flow literature, offering a fresh perspective and solution for addressing a key challenge in power systems analysis.

2. About Traditional LF Solving Methods

Load flow analysis is a fundamental task in power systems as it involves examining the grid from the perspective of power flows. Herein we will give a short summary of the problem, starting with the components of the system. A power transmission grid is composed of nodes physically realized in substations, aerial or cable lines, and transformers that connect the nodes together. The transmission grid is fed at one or more generation nodes by synchronous generators installed in power plants. The grid then feeds loads consisting of sub-transmission and distribution grids originating from substations called load nodes. Interconnection nodes are those where more than two lines converge and are used to achieve the desired mesh configuration of the grid. In studying the steady-state operation, generators and loads are usually simulated by the powers they inject or take from the nodes, constituting external constraints imposed on the grid. This simplification is possible because each component of the transmission grid [17] can be considered symmetric, with good approximation. The goal of load flow analysis is to find the nodal voltages and power flowing in the lines connecting grid nodes, considering the loads or generators at a particular time instant. During LF evaluation, active and reactive power are considered constant and given, whereas nodal and generator voltages assume the values required to satisfy the power flow need. Since LF is defined in terms of powers at nodes, it is intrinsically a nonlinear problem, which requires an iterative scheme for its solution. In traditional LF solving methods, such as the Gauss–Seidel and Newton–Raphson methods, the problem is solved iteratively by linearizing the power flow equations at each iteration. The Gauss–Seidel method works by solving the power flow equations sequentially, one node at a time, while the Newton–Raphson method solves the equations simultaneously for all nodes, using a linearized version of the problem achieved by exploiting first-order derivatives and Taylor series expansion. However, these methods can be slow and computationally intensive for large-scale systems, making the study of faster solution techniques of

interest important above all in a less stable grid due to the proliferation of renewable source plants. As a result, new and faster methods are being developed, such as the Compensation Admittance Load Flow (CALF) method, which is presented in this paper.

2.1. Load Flow Problem Formulation

In this paragraph, the formulation of the load flow problem [1,2] is expressed as simply as possible. Figure 1 shows a typical small electrical grid for load flow problems, where generators (circle) and loads (triangles) are represented by the active and reactive powers supplied and absorbed, respectively. These are connected to the grid at nodes, which, as previously stated, are called buses or busbars, since they are the busbars of electrically independent stations. The buses are connected among them by lines (power lines).

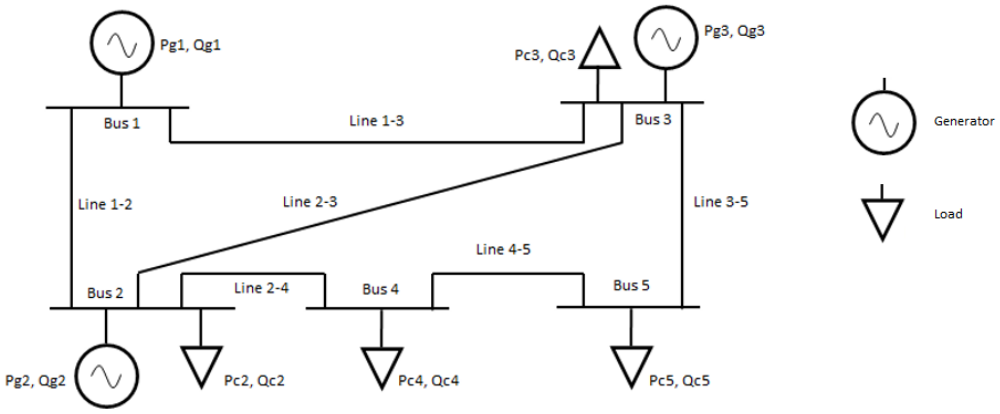

Figure 1. Typical scheme of a load flow power grid.

The load flow analysis is conducted to determine power flows on various lines and voltage on each busbar, with the aim to furnish all the users with the desired power, to guarantee that the busbars' voltages are kept within certain bounds and to prevent overloading of lines. The primary parameters of lines are assumed to be constant, with conductor resistance corresponding to an assigned operating temperature. Overhead lines are assumed to have constant transverse conductance due to small corona losses. In any case, homogeneous lines, whether overhead or cable, can be represented by using a passive two-port network satisfying reciprocity theorem conditions, which makes possible their circuital schematization as a simple π network. It is worth noticing that load asymmetries in the three phases due to non-negligible single-phase loads in LV and MV grids are compensated by grid operators [18,19], allowing for a single-phase scheme to be used for all components of three-phase grids. The external constraint conditions are expressed through node-imposed quantities. Equations governing grid operation can be written by applying Kirchhoff's principles to nodes and meshes. The neutral is counted as the second terminal shared by all the loads or generators of each busbar: in this way, it is a sort of reference node. Current and voltage are defined for each node as phasors.

For example, in a small system constituting only three busbars, and substituting the transmission lines equivalent model, it is possible to obtain the circuital representation of Figure 2. The network can be seen in this case in terms of four terminals (in the general case as a $N + 1$ terminal network, where N is the number of busbars), which allows a simple representation by means of an admittance (or impedance) matrix as follows:

$$[I_{bus}] = [Y_{bus}] \cdot [V_{bus}] \quad (1)$$

where $[I_{bus}]$ is the vector of the phasors of the current I_k (supplied) at the busbars, $[V_{bus}]$ is the vector of the phasors of the voltage V_k of the busbars, and $[Y_{bus}]$ is the admittance bus matrix. The elements of the admittance bus matrix can be easily computed by inspection, according to circuit theory. Indeed, the diagonal element (Y_{ii}) is equal to the sum of the admittance connected to node "i", whereas the other elements (Y_{ij}) are the sum, with sign

changed, of the admittance directly connecting node "*i*" and "*j*". Clearly, the admittance bus matrix is symmetric.

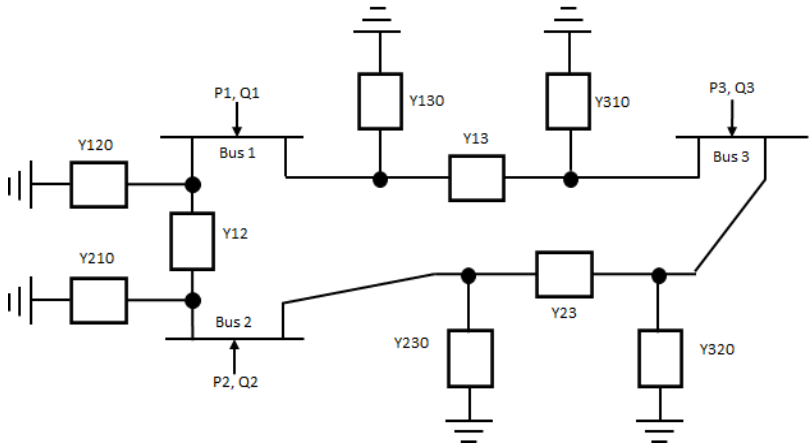

Figure 2. A three-bus power grid, considering complete lines model.

Now let us look at Equation (1), which in a less compact form becomes:

$$I_k = \sum_{n=1}^{N} Y_{kn} \cdot V_n \tag{2}$$

for each element I_k of the I_{bus} vector, each admittance Y_{kn} of Y_{bus}, and each nodal voltage of V_n vector. From voltages and currents, it is possible to compute the active and reactive power delivered by generators or absorbed by loads. For sake of clarity, let us consider a generic busbar "*k*" as in Figure 3.

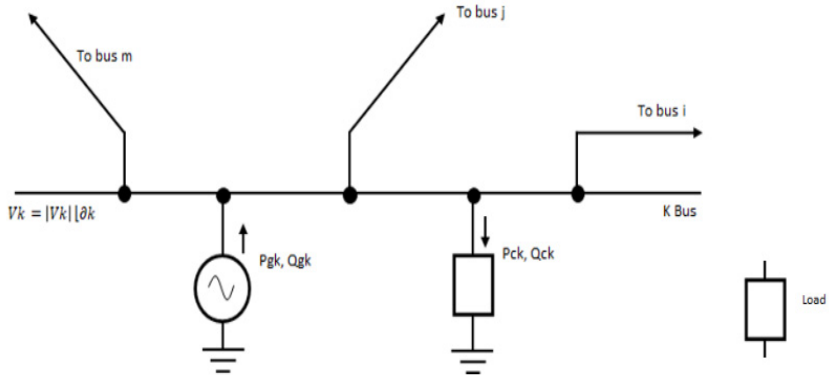

Figure 3. Detail of k-bus of Figure 1 generic grid.

The P_k and Q_k (active and reactive power) of the k bus-bar are expressed in Equation (3):

$$\begin{aligned} P_k &= P_{gk} - P_{ck} \\ Q_k &= Q_{gk} - Q_{ck} \end{aligned} \tag{3}$$

where S_k is the complex power, which can be also expressed as a function of the k-nodal voltage and current V_k and I_k (with the * we indicate the complex conjugate).

$$S_k = V_k \cdot I_k^* = P_k + jQ_k \tag{4}$$

Substituting (1) in (4) we obtain (5):

$$P_k + jQ_k = V_k \cdot \left[\sum_{n=1}^{N} Y_{kn} \cdot V_n \right]^* \tag{5}$$

with $k = 1, 2, \ldots, N$ nodes. Now considering the polar form in (6):

$$\begin{aligned} V_n &= \left|V_n\right| e^{j\partial_n} \\ Y_{kn} &= \left|Y_{kn}\right| e^{j\theta_{kn}} \end{aligned} \tag{6}$$

Then, substituting (6) in (5), we obtain (7):

$$P_k + jQ_k = V_k \cdot \sum_{n=1}^{N} Y_{kn} \cdot V_n \cdot e^{j(\partial n - \partial k - \theta kn)} \tag{7}$$

That is, applying Euler's equality in Equation (7), finally we obtain power flow equations for each bus active and reactive power in (8):

$$\begin{aligned} P_k &= V_k \cdot \sum_{n=1}^{N} Y_{kn} \cdot V_n \cdot cos(\partial_n - \partial_k - \theta_{kn}) \\ Q_k &= V_k \cdot \sum_{n=1}^{N} Y_{kn} \cdot V_n \cdot sin(\partial_n - \partial_k - \theta_{kn}) \end{aligned} \tag{8}$$

As shown in (8), the active and reactive power of each bus are related through two nonlinear algebraic equations involving the nodal voltages and the admittances of the grid. Equation (8) can be seen consequently as a system of $2N$ equations. The unknowns theoretically should be the voltages in module and phase, but really they depend on constraints. Indeed, the load flow problem involves finding the unknown voltages at each busbar for a given set of known loads (Pl, Ql) and generators (Pg, Qg). However, the total active and reactive powers are not known a priori due to line losses, which depend on the unknown voltage. To resolve this issue, one of the busbars, named the slack bus, is chosen to equilibrate the powers: the active and reactive power for f or this node are consequently derived unknowns (with this expression we indicate that this quantity is computed by knowledge of voltages), whereas the voltage are fixed at 1.0 p.u. with phase equal to zero. The Qg of generator is usually left as a derived unknown, while the voltage is fixed. In this way, we have the useful information about the values of the voltages of generators, which allow us to guarantee the correct operation of the grid. Typically, the slack bus is chosen as the busbar with the largest generation, often the secondary busbar of the transformer that feeds the grid. Table 1 shows the difference between busbars, as previously discussed.

Table 1. Types of busbars.

Type	Known Values	Unknown Parameters
Slack bus	V = 1.0 p.u., delta = 0°	P, Q
Load bus (simple gen)	Pk, Qk	V, delta
Gen bus	Pk, Vk	Q, delta

2.2. Newton–Raphson Method

The iterative Newton–Raphson [1,2] procedure is a widely used method for solving nonlinear equations, including the power flow equations in electrical power systems. The procedure involves iteratively updating the unknown voltages at each node in the system until a solution that satisfies the power flow equations is found. In order to formulate the problem, let us consider Equation (9) in general form as follows:

$$y = [P_k(x)\ Q_k(x)\ ] = [f_1(x)\ f_2(x)\ \ldots\ f_n(x)\ ] \tag{9}$$

Now, if we start with the first order expansion of the generic $f_k(x)$ in the Taylor series around x_0 and make some manipulations, we find the iterative formula for solution

$$x^{i+1} = x^i + J^{-1(i)} \cdot \left\{ y - f\left[x^i\right] \right\} \tag{10}$$

where J represents the Jacobian, defined as:

$$J^{(i)} = \frac{df(x)}{dx}|_{x=x^i} = \begin{bmatrix} \frac{df_1(x)}{dx_1} & \cdots & \frac{df_1(x)}{dx_{2N}} \\ \vdots & \ddots & \vdots \\ \frac{df_n(x)}{dx_1} & \cdots & \frac{df_n(x)}{dx_n} \end{bmatrix} \tag{11}$$

The current iteration count is represented by the i index. When $x^{(i+1)}$ varies within the predetermined tolerance limit and convergence is attained, the algorithm terminates. The convergence of the iterative Newton–Raphson procedure depends on the choice of initial guess values and the condition of the Jacobian matrix. In some cases, the procedure may fail to converge and other methods could be required to find a solution. Once a solution is found, the active and reactive power flows at each node, as well as the corresponding losses in the system, can be calculated. These values are important for the operation and planning of the power system, as they inform decisions on system upgrades, maintenance, and dispatch of generation resources.

2.3. Gauss Seidel Method

The Gauss–Seidel method [1,2] is a popular iterative method for solving power flow equations in power systems. It can be used to solve linear systems in matrix form, which arise from the power flow equations in the form of (5). The method is based on the idea of solving one equation at a time and updating the solution as soon as possible. The algorithm involves setting up an iterative process to solve the power flow equations. The process begins by assuming all busbar voltages are equal to 1 + j0 p.u., which is known as the flat start assumption. The nodal voltages are then computed using the equation:

$$V_k = \frac{1}{Y_{kk}} \left[\frac{P_k - jQ_k}{V_k{}^*} - \left(\sum_{n=1}^{k-1} Y_{kn} \cdot V_n + \sum_{n=k+1}^{N} Y_{kn} \cdot V_n \right) \right] [V] \tag{12}$$

Equation (12) is obtained by (5) arranging terms in the function of the nodal voltage at k-busbar V_k iteratively. From the calculation of the previous i iteration, a more accurate estimate is obtained and so on until ${V_k}^{(i+1)} - {V_k}^{(i)}$ is less than a set tolerance. The algorithm's processes involve calculating the overall powers at each bus, creating the Y_{bus}, and solving the power flow equations iteratively until convergence is obtained below a predetermined tolerance. While the Gauss–Seidel method has advantages in terms of its simplicity and ease of implementation, it converges slowly, which is a drawback for power systems with many busbars. To speed up convergence, an alpha-factor can be introduced, with a value that varies between 1.5 and 1.7. However, for grids with many known factors, the Newton–Raphson method is more suitable, as it requires a fixed number of iterations approximately independent of the number of nodes. It is important to note that as the number of nodes increases, so do the number of iterations and calculation time for the Gauss–Seidel method.

2.4. Differences between NR and GS

It is important to note that both methods have their own advantages and limitations, and the choice of method depends on the specific characteristics of the power system being analyzed. For small power systems, the NR method is generally preferred due to its faster convergence and higher precision. However, for large power systems with hundreds or thousands of nodes, the G-S method may be more suitable due to its lower memory requirements and simpler implementation. In practice, a combination of both methods may be used, such as using the a method for initial solutions and then switching to the other for faster convergence in subsequent iterations.

3. Compensation Admittance Load Flow (CALF): A New Linear Load Flow Solving Method

Compensation Admittance Load Flow is the new iterative load flow method proposed in this paper. Its aim is to combine the advantages of NR and GS methods within a certain tradeoff for software complexity implementation to be kept as simple as possible. In the next paragraph, CALF method is illustrated through a circuital example.

CALF Method

Let consider the simple network in Figure 4 in order to illustrate how CALF works:

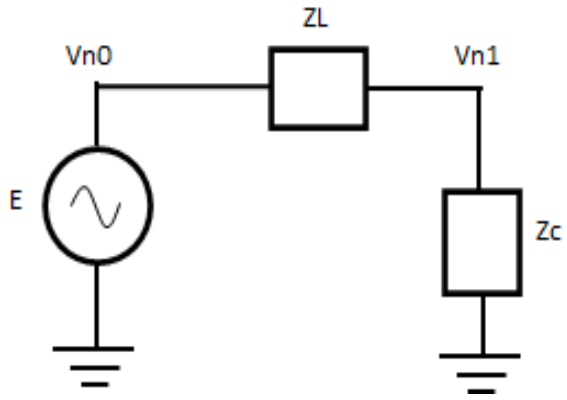

Figure 4. A simple grid to show CALF method improvement.

The circuit consists of a voltage source with E = 220 + 0j $[V]$, a line impedance Z_L = 0.01 + 0.003j [Ω], and a load impedance Z_c = 1 + 0.01j [Ω]. Using Ohm's law, the current flowing through the circuit can be calculated as:

$$I = \frac{E}{Z_L + Z_c} = 217.8 - 2.803j\ [A] \tag{13}$$

The voltage at node 1, V_{n1}, can then be calculated as:

$$V_{n1} = I \cdot Z_c = 217.8 - 0.6253j\ [V] \tag{14}$$

The complex power consumed by the load, S_c, can be calculated as:

$$S_c = V_{n1} \cdot I^* = 47438.46 + 474.38j\ [VA] \tag{15}$$

To introduce the CALF method, there is the need to view the same problem from the perspective of power flow. The CALF method is based on the assumption that loads and generators can be modeled as current sources with shunt admittance (that is, as a Norton equivalent bipole). This simplifies the power flow equations and allows for a faster and more efficient solution compared to traditional methods such as the NR and GS methods. In this context, the circuit diagram in Figure 4 can be represented in the form shown in Figure 5:

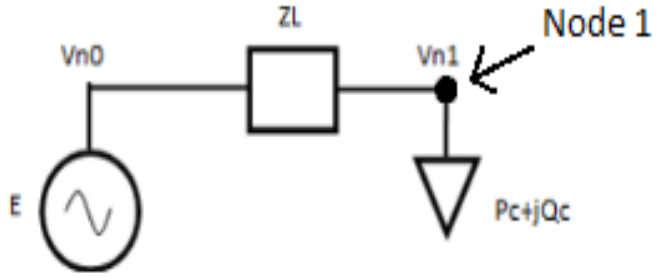

Figure 5. A simple grid to show CALF method improvement, in load flow notation.

Additionally, let E (transformer generator), Z_L (line impedance), and S_c (load) be $E = 220 + 0j$, $Z_L = 0.01 + 0.003j$, and $S_c = 47{,}438.46 + 474.38j$, respectively. Assume, as defined and desired in all electrical grids, that the voltage on the load V_n is equal to the nominal voltage, equal to the one of the bus bar E, that is, $V_{n1} = E = 220 + 0j\ [V]$ as the initial guess value condition equal for all nodes, called the flat start. Typically, the nominal voltage is considered as the value for the flat start. Now, let us try to linearize the problem. To do this, the generator at the bus bar (or slack bus) can be modeled as a current generator equal to I_{gv} (16):

$$I_{gv} = \frac{E}{Z_L} \tag{16}$$

On the other hand, even the load absorbing S_c can be seen like a current generator draining from node 1, the following load current I_c:

$$I_c = \left(\frac{S_c}{V_{n1}} \right)^* \tag{17}$$

The circuital diagram becomes the following shown in Figure 6 considering the introduction of current equivalent generators:

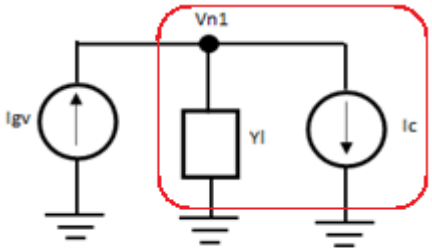

Figure 6. The simple grid, transformed after CALF linearization process.

Then, using Millmann's method at the node V_{n1}, it is possible to obtain:

$$V_{n1} = \frac{I_{gv} - I_c}{Y_L} \tag{18}$$

Then, finally, we obtain the load complex power in (19):

$$S_c = V_{n1} \cdot I_c^* \tag{19}$$

However, V_{n1} in (19) assumes a new value that the initial guess value assumed before. Indeed, by computing the Formulas in (14)–(17), it is possible to obtain the following results in Table 2:

Table 2. Sample grid values vs. iteration number at very first iteration.

Iteration	I_g	I_c	V_{n1}	S_c
0	-	-	220 + j0	-
1	20,183.48 − 6055.04j	215.629 − 2.15629j	217.8372 − 0.625325j	46,973.4 + 334.8826j
2	-	-	-	-
3	-	-	-	-
4	-	-	-	-

From the calculations performed, it can be highlighted that:

1. The voltage at node V_{n1} (considering the flat start value) decreased from 220 V in-module to 217.83 V in-module. Moreover, it is underestimated compared to the 217.80 V calculated with the exact Millman method.
2. The apparent power absorbed by the load equal to 46.97 kVA is underestimated if compared to the one equal to 47.44 kVA obtained with the exact Millman method.

To improve the accuracy of the results and ensure the convergence of the proposed method, the fundamental concept of "compensating admittance" was introduced. This concept is pivotal in refining the load flow calculations, addressing discrepancies in power generation and consumption, and ultimately ensuring that the method aligns closely with the expected behavior of the electrical network. This compensating admittance signifies the admittance that absorbs/releases the power difference lacking in the load's current generator, when subjected to the freshly calculated nodal voltage, relative to the anticipated complex power on the load derived from the problem data. The compensating admittance, denoted as Y_c, is a key component that acts as an "equilibrating factor" to rectify any mismatches between the actual power flow in the network and the power values anticipated based on the initial problem data. Think of Y_c as a virtual entity that plays a crucial role in balancing the power equations at each individual node in the network. Imagine a situation where iterative calculations yield power values at a specific node (S_{ce}) that do not perfectly align with the power values expected according to the initial problem data (S_c). This discrepancy in power, aptly represented by S_d, signifies the "unaccounted for" or the "deviation" between the complex power calculated from the previous iteration and the power value expected at that node based on the problem data. In summary, Y_c is an indispensable element in our method, fine-tuning the calculations to harmonize with the expected power values from the problem data, and S_d quantifies the extent of the power difference that Y_c effectively addresses. This approach significantly enhances the accuracy of load flow calculations, culminating in results that align closely with the actual behavior of the electrical network. This core concept of the proposed and analyzed method in this article is depicted in Figure 7:

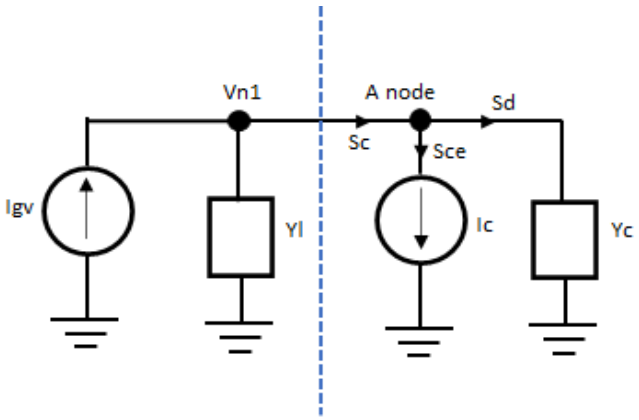

Figure 7. The sample grid after introducing the compensation admittance.

From Figure 7, by adapting the current representation, it can be deduced that the sum of powers at node A is equal to:

$$S_c = S_{ce} + S_d \tag{20}$$

where S_d is thus the difference between the power given in the problem data S_c and estimated in iteration power at the nodes S_{ce}. Here, S_d signifies the power difference between the power provided in the problem (S_c) and the power estimated during node iteration (S_{ce}). S_d serves as the quantification of the difference between the complex power calculated in the previous iteration (S_{ce}) and the complex power expected at that node based on the original data (S_c). In essence, S_d represents the "error" or "delta" between the iterative power calculations and the power values anticipated according to the given problem. Here is where the significance of Y_c becomes evident: Y_c is a value that was determined based on S_d, and its role is to "absorb" or "supply" this power difference, thereby bringing the calculations closer to the expected power values. Y_c takes the form of a complex value (admittance) that is meticulously designed to precisely compensate for the deviation between the iterative power calculations and the power values that were anticipated from the problem data. By leveraging Y_c, the calculations are tuned for nodal

voltage, making them more precise by accounting for the power difference (S_d). This iterative process, which involves the consideration of Y_c, continues until convergence. Convergence indicates that the calculated values are in remarkable agreement with the expected power values, thus ensuring that the method accurately reflects the real-world behavior of the electrical network. In other words, S_d signifies the difference between the complex power calculated from the previous iteration and S_{ce}, which represents the expected complex power at the node according to the problem data. Consequently, it is possible to derive the compensating admittance value Y_c (19), which absorbs/supplies this S_d power difference:

$$Y_c = \frac{S_d^*}{|V_{n1}^2|} \tag{21}$$

To gain a deeper grasp of the iterative process, the earlier defined Table 2 can be extended to Table 3, incorporating the new S_d and Y_c values. Through subsequent iterations until achieving convergence, the presence of Y_c is factored in when calculating nodal voltage. As a result, Equation (21) is revised as follows:

Table 3. Sample grid complete values vs. iteration number.

Iteration	I_g	I_c	V_{n1}	S_c	S_d	Y_c
0	-	-	220 + j0	-	-	0 + 0j
1	20,183.48 − 6055.04j	215.629 − 2.15629j	217.8372 − 0.625325j	46,973.4 + 334.8826j	10.1328 + 0.101328j	0.000213624 − 2.1362×10^{-6}j
2	-	-	-	-	-	-
3	-	-	-	-	-	-
4	-	-	-	-	-	-

So, at this point, it is possible to iterate over and over until the desired tolerance on nodal voltage for the difference from two adjacent iterations is reached. This condition is expressed in (22):

$$\left| \frac{V_{n1}^i - V_{n1}^{i-1}}{V_{n1}^{i-1}} \right| > tol \tag{22}$$

where i represents the actual iteration number and tol the fixed tolerance. To summarize, the CALF method uses the concept of compensating admittance to adjust the power absorbed/supplied by a node and ensure that the node power matches the expected value from the problem data. The method iteratively calculates the nodal voltages using the compensating admittance term until the desired tolerance on the difference between two adjacent iterations is reached. At the first iteration, the compensating admittance is considered null, and it can be applied to both generation and load nodes. This approach keeps the method linear and allows for fast calculation, while also increasing precision by reducing approximations in power estimations.

4. CALF vs. Traditional Methods: Tests and Results

In this section, a comprehensive comparison between the results achieved through the Compensation Admittance Load Flow (CALF) method and those obtained from well-established traditional load flow techniques such as the Newton–Raphson (NR) and Gauss–Seidel (GS) methods is introduced. The objective is to evaluate the performance of the CALF method across various scenarios, specifically using three distinct ENEL grids: a binodal grid (referred to as "grid2"), a 19-node grid (designated as "grid19"), and a larger 101-node grid (referred to as "grid101"). The analysis began by benchmarking the exact solution attained through the Millman approach on the binodal grid. Then the solutions generated using the CALF, NR, and GS methods for this particular grid were juxtaposed. This direct comparison provides insights into the advantages and capabilities of the proposed CALF method compared to the traditional approaches. Subsequently, a comparative study to

encompass the computational time required by each method to compute solutions for all three standard grids was conducted. This evaluation of computational efficiency is essential in practical applications and is often a significant factor in determining the feasibility of a load flow method. A clear overview of the time efficiency of the CALF method compared to NR and GS for each grid size was provided. Importantly, the simulations were initially performed in the context of the BT domain, but the applicability of this approach is not limited to it, as it potentially extends to medium-voltage (MT) and high-voltage (AT) scenarios as well. This demonstrates the versatility of the CALF method and its potential to address load flow challenges across different voltage levels, making it wellsuited for the typical BT and MT network scenarios in Italy. Additionally, the method's adaptability to the AT domain showcases its scalability and potential for broader application in more complex power systems. Following this, an in-depth comparison evaluating the precision of various parameters, including nodal voltages, active power, reactive power, and the deviation from nominal voltage, was described. This comparison was conducted between the CALF-NR and GS-NR methods for the three standard grids (grid2, grid19, and grid101). This thorough assessment provides a comprehensive understanding of the performance and accuracy of the CALF method in comparison to traditional methods. Additionally, diverse simulation scenarios were explored by testing cascaded methods (GS-NR) and load flow analyses incorporating different initial guess values (GS-NR-CALF). This exploration allows us to gain valuable insights into how these methods respond when applied to different standard grids and how the initial guess values impact their convergence. Overall, this multifaceted comparison provides a comprehensive understanding of the strengths, limitations, and nuances of our CALF method, shedding light on its performance across different grid sizes and highlighting its potential for broader applicability in both medium- and high-voltage scenarios. The aim is to provide readers with a clear and detailed assessment of the capabilities of the CALF method, showcasing its distinct advantages and contributions in the field of load flow analysis. This comprehensive comparison underscores the adaptability of theCALF method to Italian BT and MT network scenarios, as well as its potential extension to the more complex AT domain, addressing the reviewer's request for a thorough explanation of the method's adaptability to various network scenarios.

4.1. Methods Solution vs. Exact Solution

To rigorously assess the precision and effectiveness of the CALF (Compensating Admittance Load Flow) method, a comprehensive comparative analysis alongside well-established traditional load flow techniques, namely the Gauss–Seidel (GS) and Newton–Raphson (NR) methods, was introduced. The objective is to showcase how CALF outperforms these traditional approaches, particularly under specific scenarios, with a focus on grids of varying sizes. This comparison allows us to not only highlight the strengths of CALF but also to emphasize its potential applicability beyond the low-voltage (BT) domain, extending its scope to medium-voltage (MT) and high-voltage (AT) scenarios. This evaluation starts with a well-defined and standard grid, referred to as "Grid2" (as depicted in Figure 8), with clearly specified circuit element values. These values are as follows: source voltage (E) = 220 + 0j.

Load parameters:

Y0 = $-0.20637544213001807 + 0.00023461000255635677$j (signifying power injection into the node, e.g., from renewable distributed energy);

Y1 = $0.15118310047933142 + 5.046264405831989 \times 10^{-5}$j;

YL = $6.554726 - 0.21349$j;

Yi = $51.65289256198347 - 51.65289256198347$j.

By leveraging this precisely defined grid configuration, the complex power for the loads using the current nodal method was computed. This computation results in a load flow equivalent representation of the problem, as illustrated in Figure 9.

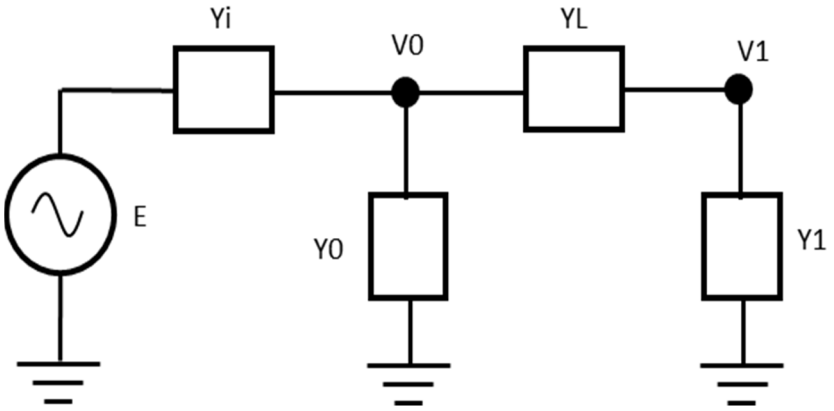

Figure 8. Grid2 admittance representation.

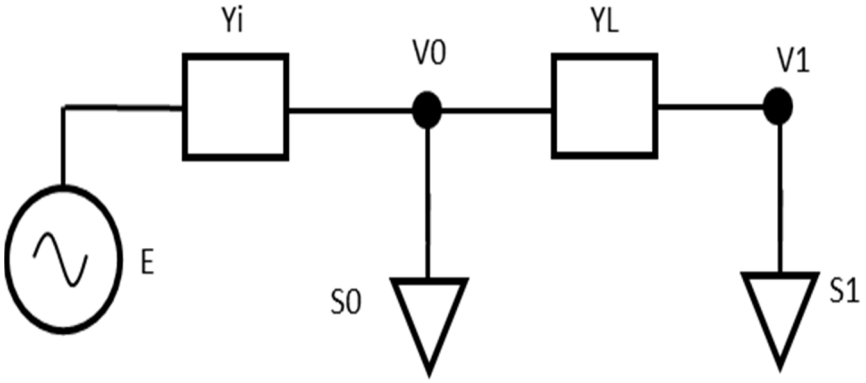

Figure 9. Grid2 load flow representation.

Where the bus powers are:
S0 = −10,000 VA;
S1 = 7000 VA.

With this groundwork in place, the load flow problem can be solved using the three methods: CALF, GS, and NR. Then it is possible to compare their respective solutions to the exact solution obtained from the known standard grid configuration. The primary focus is on key physical quantities, and the main results are shown in Tables 4–6.

Table 4. Exact solutions vs. CALF solutions.

Node Number	Exact Solutions	Calf Solutions
	NA	3
Iteractions	NA	997800
Exec. time (ns)	[220.12516083 + 0.1245588j	[220.12407684 + 0.12468541j
Complex node voltages	215.16765754 − 0.03769608j]	215.1582232 − 0.03557047j]
ABS nodal boltages	[220.12519607 15.16766084]	[220.12411215 215.15822614]
P.U. ABS nodal voltages	[1.00056907 0.97803482]	[1.00056415 0.97799194]
Line current	32.529 + 0.0051589j	32.584 − 0.00972j
Transf. current	−12.8987 + 0.0310966j	[−12.84928 − 0.0314343129j
Expected CPLX pow. @ buses	[−10000. + 0.j 7000. + 0.j]	[−10000. + 0.j 7000. + 0.j]
Computer CPLX pow. @ buses	[−9999.923 − 22.6850j	[−10000.304 − 0.27694j 7003.331 +
Transf. CPLX power	6999.341 − 4.78876j]	0.30975j]
Transf. losses	−2837.116 + 6.9064j	−2836.600 + 6.77951j
LINES LOSSES	1.6182 + 1.60275j	1.5903798 + 1.606019j
	161.2653 + 5.30368j	161.809 + 5.17349243j

Table 5. Exact solutions vs. GS solutions.

Node Number	Exact Solutions	GS Solutions
Iterations	NA	3
Exec. time (ns)	NA	996700
Complex node voltages	[220.12516083 + 0.1245588j	[220.12400151 + 0.12854805j
ABS nodal voltages	215.16765754 − 0.03769608j]	215.1664764 − 0.03288369j]
P.U. ABS nodal voltages	[220.12519607 215.16766084]	[220.12403905 215.16647891]
Line current	[1.00056907 0.97803482]	[1.00056381 0.97802945]
Transf. current	32.529 + 0.0051589j	32.529684 − 0.000238j
Expected CPLX pow. @ buses	−12.8987 + 0.0310966j	−13.0449 − 0.234841j
Computed CPLX pow. @ buses	[−10000. + 0.j 7000. + 0.j]	[−10,000. + 0.j 7000. + 0.j]
Transf. CPLX power	[−9999.923 − 22.6850j	[−10,000. + 0.j 7000. + 0.j]
Transf. losses	6999.341 − 4.78876j]	−2837.1458 + 6.95615j
Line losses	−2837.116 + 6.9064j	1.5874 + 1.706019j
	1.6182 + 1.60275j	161.2667 + 5.25014j
	161.2653 + 5.30368j	

Table 6. Exact solutions vs. NR solutions.

Node Number	Exact Solutions	NR Solutions
Iterations	NA	2
Exec. time (ns)	NA	10597000
Complex node voltages	[220.12516083 + 0.1245588j	[220.13196038 + 0.13207919j
ABS nodal voltages	215.16765754 − 0.03769608j]	215.28290759 + 0.02538032j]
P.U. ABS nodal voltages	[220.12519607 215.16766084]	[220.132 215.28290909]
Line current	[1.00056907 0.97803482]	[1.0006 0.97855868]
Transf. current	32.529 + 0.0051589j	31.8069 − 0.33584j
Expected CPLX pow. @ buses	−12.8987 + 0.0310966j	−13.638407 − 0.00613718j
Computed CPLX pow. @ buses	[−10000. + 0.j 7000. + 0.j]	[−10000. + 0.j 7000. + 0.j]
Transf. CPLX power	[−9999.923 − 22.6850j	[−10000. + 0.j 7000. + 0.j]
Transf. losses	6999.341 − 4.78876j]	−2843.931 + 3.5674239j
Line losses	−2837.116 + 6.9064j	1.7989 + 1.80215j
	1.6182 + 1.60275j	154.269 + 1.765264j
	161.2653 + 5.30368j	

What becomes immediately apparent from the detailed comparisons in Tables 4–6 is that a significant portion of the computed results using the grids closely aligns with the exact solution, confirming the overall accuracy of the methods. Notably, the CALF method stands out with its exceptional precision when contrasted with the NR and GS methods. This is a pivotal point to emphasize in the evaluation. However, the full extent of the superiority of the CALF method is highlighted in Table 7, where we delve deeper into the comparison, focusing specifically on the P.U. ABS nodal voltages. This table provides a detailed view of the deviation in each method's results from the exact values, presenting this discrepancy as a percentage. It also presents the average percentage distance from the exact values for each method.

Table 7. Comparison of P.U. ABS nodal voltages for different methods.

Node Number	Exact SOL.	CALF	GS	NR
[Node 1 Node 2] in p.u.	[1.00056907 0.97803482]	[1.00056415 0.97799194]	[1.0006 0.97855868]	[1.00056381 0.97802945]
Distance % from exact values [Node 1 Node 2]	//	[−0.0004917 −0.004384]	[0.0030912 0.05356]	[−0.0005257 −0.000549]
Distance % from exact value Node means	//	−0.002438	0.028327	−0.000537

This detailed analysis of Table 7 unequivocally demonstrates that the CALF method consistently yields more accurate results when compared to the traditional GS and NR methods. The ability of CALF to deliver superior precision in nodal voltages is a key distinguishing feature, signifying its efficacy, particularly in scenarios with low to medium node counts. This aspect of the results serves as a strong testament to the advancements provided by the CALF method. In conclusion, the comprehensive comparison showcases not only the precision but also the superiority of the CALF method over traditional load flow techniques, thereby reinforcing its potential to be a valuable solution for power system analysis in Italian BT and MT scenarios, with an extension to AT scenarios.

4.2. Method Solution vs. Execution Time

In this section, an in-depth exploration of the execution time, a pivotal facet in evaluating the prowess of the CALF method in comparison to traditional approaches, is presented. Let consider grid sizes spanning 2, 19, and 101 nodes, seeking to provide a comprehensive understanding of the temporal efficiency of the Gauss–Seidel (GS), CALF, and Newton–Raphson (NR) methods. The consolidated results are neatly encapsulated in Table 8, serving as a valuable reference to discern execution time trends across these distinctive grid configurations. To visually elucidate the temporal dynamics of these methods, the results are presented in a graphical format, as depicted in Figure 10.

Table 8. Execution time (ms) for different methods on different grids.

Node Number	GS	CALF	NR
2	0.9967	0.9978	3.7756
19	9.739739	10.44369	19.93895
101	39.54172	17.9522	20.02764

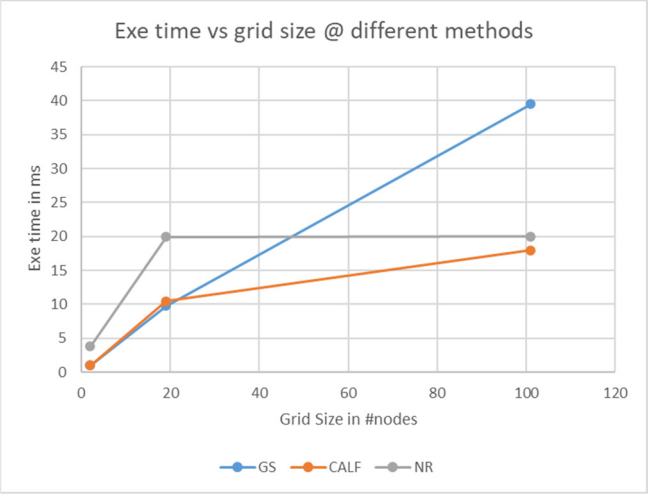

Figure 10. Representation of execution time for different methods on grids.

The discerning reader will observe that the CALF method demonstrates remarkable prowess in realizing its primary objective of time efficiency. When confronted with grids featuring 2 and 19 nodes, the Gauss–Seidel (GS) method marginally outperforms CALF in terms of execution speed. However, the competitive landscape undergoes a significant transformation when confronted with larger grids, such as the 101-node scenario. Here, CALF emerges as a clear winner, exhibiting substantial gains in execution time over both the GS and NR methods. This pronounced advantage in execution time firmly positions CALF as an attractive alternative, particularly when grappling with complex load flow challenges within substantial grid infrastructures. The implications of these findings are significant, demonstrating CALF's capacity to effectively handle intricate scenarios while optimizing time efficiency, a pivotal consideration in real-world power system analysis.

4.3. Execution Time vs. Combined Methods

In this section, a comprehensive analysis of the results achieved through the implementation of combined methods is reported (Figure 11). The approach begins with the execution of the CALF method on a given grid and subsequently leverages the Newton–Raphson (NR) and Gauss–Seidel (GS) methods, initializing them with the outcomes obtained from the CALF run. This strategy allows us to explore the performance of CALF when compared to these established traditional methods while also assessing the combined effects of utilizing CALF as a starting point. The primary focus revolves around a detailed comparison of the nodal voltages obtained through the CALF-NR and CALF-GS methods. To provide a comprehensive overview, this comparison was conducted on three standard grid sizes: a small-scale grid with 2 nodes, a moderate 19-node grid, and a larger grid with 101 nodes. Additionally, we meticulously examined the deviations from the nominal voltage, alongside evaluating the active and reactive power values to gain a holistic perspective on the methods' performances. The results of this analysis are summarized in Table 9, showcasing the execution times (in milliseconds) for the different combined methods applied to the specified grid sizes:

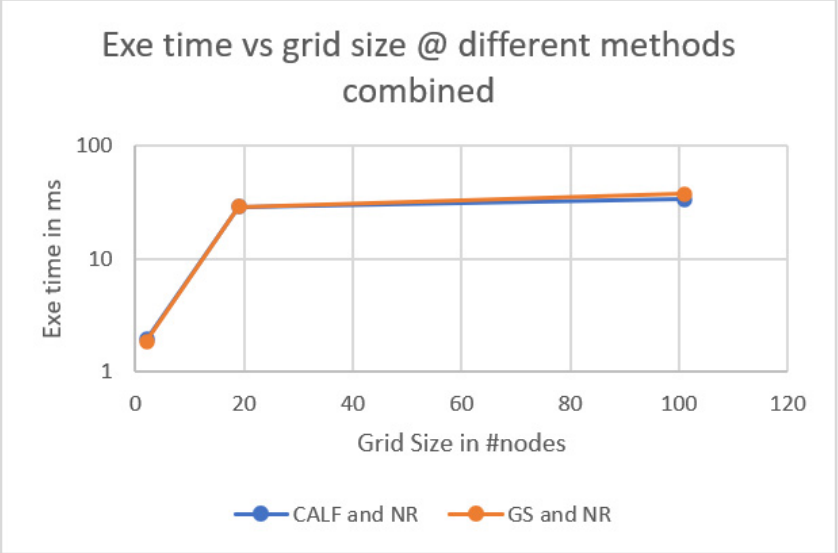

Figure 11. Representation of execution time for different combined methods on grids.

Table 9. Execution time (ms) for different combined methods on different grids.

Node Number	CALF and NR	GS and NR
2	1.9245	1.8529
19	28.835	28.786
101	33.5724	37.5614

The insights gleaned from these results offer a profound understanding of CALF's comparative advantages, particularly against the traditional NR and GS methods:

Execution time efficiency: The analysis of execution times unequivocally reveals CALF's prowess in speed. Across all grid sizes, CALF exhibits superior execution times when contrasted with the NR and GS methods. This efficiency becomes notably pronounced when dealing with larger grids, where CALF's capabilities shine, showing a clear advantage in handling complex scenarios.

However, the story is not limited to individual method performance; the combined application of CALF with NR and GS must be considered:

Combined performance: While CALF stands out as a swift individual performer, the results do indicate that the combination of CALF with the traditional methods (CALF-NR and CALF-GS) leads to slightly inferior outcomes. This can be attributed to the "combined

time execution effect", a factor that introduces a degree of overhead when integrating multiple methods. Despite this, it is essential to emphasize that CALF still serves as a highly valuable alternative for load flow analysis. This is especially true when dealing with larger grids, where the execution time of traditional methods, such as NR and GS, can become prohibitively high.

These findings underscore CALF's value as a time-efficient solution for load flow analysis, particularly in scenarios involving substantial grid sizes. They reinforce the overarching objective of CALF, which is to surpass the limitations of traditional methods, providing a competitive alternative in terms of both speed and accuracy.

4.4. Precision vs. Methods and Grids

In this section, the focus lies on critical parameters such as nodal voltages, active power, and reactive power. These parameters were subjected to rigorous testing across three distinct grid sizes: the compact 2-node grid, the intermediate 19-node grid, and the more expansive 101-node grid. Through this comprehensive evaluation, we compared the performance of the CALF, Newton–Raphson (NR), and Gauss–Seidel (GS) methods, ultimately drawing insightful comparisons among their results.

4.4.1. Nodal Voltage % Average Detachment vs. NR Results

In this section, the analysis of the precision tests conducted on nodal voltages, active power, and reactive power is introduced. These tests encompass a systematic evaluation of these parameters across three distinct grid sizes: 2, 19, and 101 nodes. The aim is to assess the accuracy and performance of the CALF, NR, and GS methods, comparing their results. To initiate these precision tests, the nodal voltages, active power, and reactive power were computed for each of the specified grid sizes using all three methods: CALF, NR, and GS. Subsequently, the results obtained from these methods were subjected to detailed comparison and analysis to gauge their consistency and accuracy. We present the results of the percentage detachment test, focusing on nodal voltages with respect to the NR results. The outcomes of this test are elucidated through Table 10, which outlines the average percentage detachment of nodal voltages calculated using the CALF and GS methods when compared to the benchmark NR results for the same grid configurations.

Table 10. Nodal voltage % average detachment for different methods and grids referring to NR as the most precise method.

Node Number	CALF	GS
2	101.1100482	101.1100146
19	100.3998917	100.6123748
101	101.2733728	101.5968205

Table 10 stands as a testament to this evaluation, showcasing the percentage detachment figures for nodal voltages. Through a meticulous examination of CALF and GS results, their divergence from the NR-derived results for corresponding grid sizes was obtained. The intricate interplay of these values provides a granular understanding of how CALF and GS methods perform in comparison to the rigorously accurate NR method.

The insights from Table 10 are visually encapsulated in Figure 12, an illustrative representation of the nodal voltage percentage detachment from NR results. This visual depiction distills the comparative performance of CALF and GS methods, allowing for a quick yet insightful grasp of their precision levels.

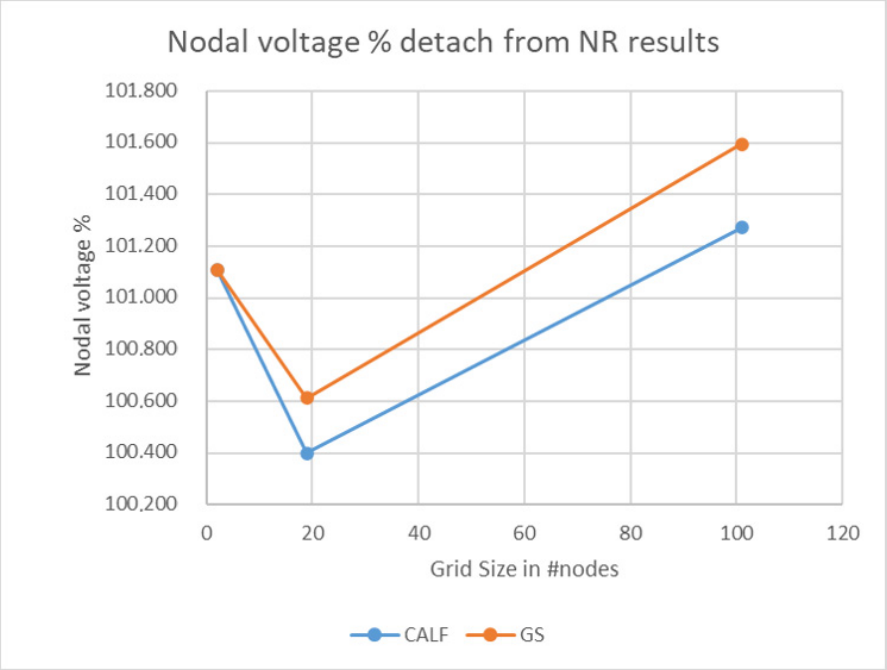

Figure 12. Representation of nodal voltage % detachment from NR results.

Upon parsing the results, a compelling narrative emerges. It becomes apparent that the CALF method outshines the GS method, showcasing enhanced precision in nodal voltage calculations. More notably, CALF's performance aligns favorably with the gold standard set by the NR method. This is a significant achievement, highlighting CALF's prowess in delivering comparable levels of precision to the well-established NR method while retaining its inherent efficiency advantage.

In summation, the outcomes of this percentage detachment test bear witness to CALF's ability to provide accurate nodal voltage calculations. By offering results that are not only more precise than the GS method but also akin to the NR method, CALF underlines its potential as a robust and efficient alternative. This precision, coupled with its expedited computational speed, positions CALF as a valuable tool for power system analysis, particularly in scenarios where time-sensitive decision making is paramount.

4.4.2. Nodal Voltage % Average Detachment vs. Nominal Voltage

Furthermore, the analysis was extended to encompass the percentage detachment test in relation to the nominal voltage. In this case, Table 11 offers an overview of the average percentage detachment of nodal voltages for the CALF, GS, and NR methods when compared to the nominal voltage for the grid sizes in question.

Table 11. Nodal voltage % average detachment for different methods and grids referring to nominal voltage.

Node Number	CALF	GS	NR
2	100.06	100.0564146	100.0563814
19	99.81	99.79562822	100.0068325
101	99.69761905	99.67897347	99.9973289

Figure 13 supplements this data by providing a graphical representation of the percentage detachment of nodal voltages from the nominal voltage. The results depicted in Table 11 and Figure 13 collectively reveal that the CALF method outperforms the GS approach in terms of nodal voltage precision, though it falls slightly behind the NR method. It is important to note that this test represents an average detachment and that deviation from

nominal voltage is inevitable due to the nature of the initial values. The higher detachment observed in CALF and GS methods when compared to NR underscores their simplicity and lower precision, although exceptions might arise based on specific grid topologies.

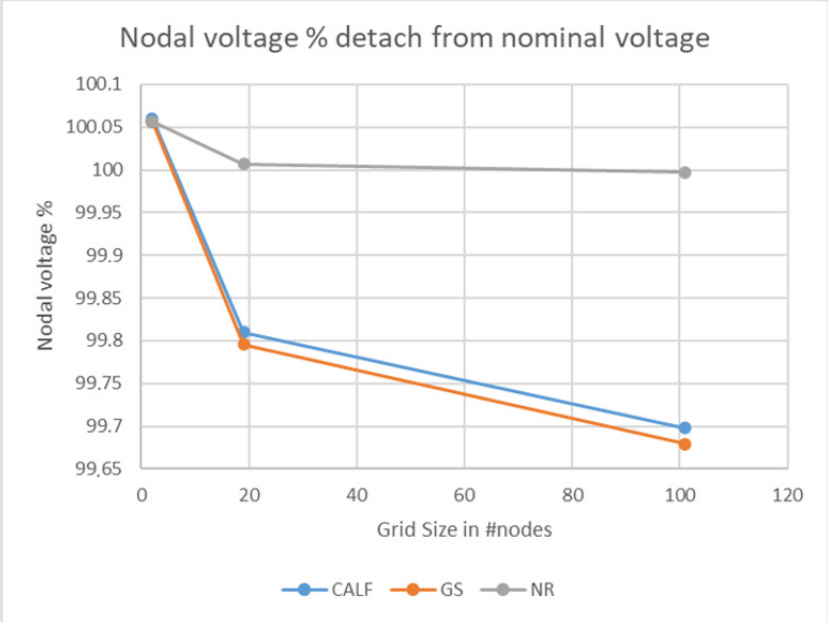

Figure 13. Representation of nodal voltage % detachment from nominal voltage.

4.4.3. Active Power Average Detachment vs. Active Power from Grid Data

In this section, the precision of active power calculations was studied. Specifically, the focus was on the active power detachment test, which involves comparing the calculated nodal active power values using the CALF, GS, and NR methods to the known active power supplied at the grid's slack bus. This evaluation was conducted across varying grid sizes, namely 2, 19, and 101 nodes. The objective was to assess the accuracy and effectiveness of these methods in reproducing the supplied active power values. The results of this active power detachment test are presented comprehensively in Table 12. This table showcases the average percentage detachment of nodal active power values for each of the methods—CALF, GS, and NR—across the specified grid sizes. These detachment percentages were calculated concerning the active power supplied at the grid's slack bus, which serves as a benchmark for comparison.

Table 12. Active power average detachment in % for different methods and grids referring to expected problem data and grid slack bus supplied active power.

Node Number	Slack Active Power [kW]	CALF% Detachment	GS% Detachment	NR% Detachment
2	14	0.0016%	0.0117%	0.0011%
19	19.6	0.0166%	0.0534%	0.0053%
101	194	0.0806%	0.0965%	0.0119%

Figure 14 complements these results by providing a visual representation of the percentage detachment of nodal active power values from the slack bus supplied active power. The graph vividly illustrates the variation in detachment percentages across the grid sizes for all three methods. Upon scrutinizing the data presented in Table 12 and Figure 14, a clear trend emerges. The CALF method consistently demonstrates higher precision compared to both the GS and NR methods for all grid sizes. Notably, as the grid size expands, the efficiency of the CALF method decreases while both the GS and NR methods become more effective in terms of precision. This trend is particularly evident in

the provided slack bus supplied active power values. The graph in Figure 14 showcases the nodal active power % detachment from nominal power. This visual representation underscores the remarkable precision of the CALF method in comparison to the GS and NR methods, especially for smaller grid sizes. However, it is noteworthy that, as indicated in the table, the precision of CALF slightly diminishes with increasing grid size, while the GS and NR methods become comparatively more accurate. In summary, the results gleaned from these active power detachment tests underscore the superior precision of the CALF method, particularly for small to medium-sized grids. While CALF demonstrates remarkable accuracy, its effectiveness might vary with grid size, with the GS and NR methods proving more efficient for larger grid configurations.

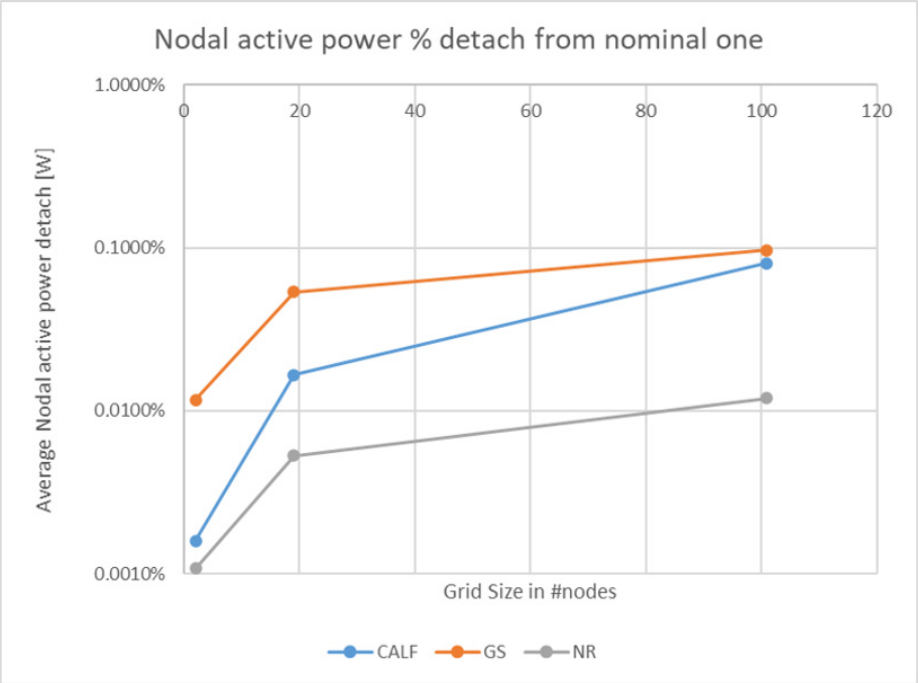

Figure 14. Representation nodal active power % detachment from slack bus supplied active power.

4.4.4. Reactive Power Average Detachment vs. Active Power from Grid Data

In this portion of the analysis, the examination was extended to encompass reactive power calculations, mirroring the methodology applied in the previous Section 4.4.3. The focus remains on the detachment test, where the precision of nodal reactive power calculations is evaluated across varying grid sizes (2, 19, and 101 nodes) using the CALF, GS, and NR methods. The objective is to assess how accurately these methods can replicate the reactive power supplied at the grid's slack bus. The outcomes of this reactive power detachment test are comprehensively presented in Table 13. This table provides a comprehensive breakdown of the average percentage detachment of nodal reactive power values for each method—CALF, GS, and NR—across the specified grid sizes. These detachment percentages were calculated in relation to the reactive power supplied at the grid's slack bus, serving as a reference point for precision assessment.

Table 13. Reactive power average detachment in % for different methods and grids referring to expected problem data and grid slack bus supplied reactive power.

Node Number	Slack Reactive Power [VAr]	CALF% Detachment	GS% Detachment	NR% Detachment
2	38.93	7.0288%	5.7494%	0.4214%
19	176.86	5.6012%	7.7929%	1.2601%
101	2565	5.6893%	4.5030%	0.9791%

Figure 15 complements these findings by providing a graphical representation of the percentage detachment of nodal reactive power values from the slack bus supplied reactive power. The graph visually illustrates the trend in detachment percentages across varying grid sizes for all three methods. Upon thorough examination of the data presented in Table 13 and Figure 15, certain patterns and observations emerge. The CALF method consistently achieves higher precision in reactive power calculations compared to the traditional GS and NR methods. Notably, as the grid size increases, the precision advantage of the CALF method over NR diminishes, albeit CALF remains superior to GS in terms of precision. These findings imply that CALF is a highly effective method for grids ranging from 10 to 80 nodes, showcasing its adaptability and accuracy in handling reactive power calculations. In summary, the results of the reactive power detachment test, as portrayed in Table 13 and Figure 15, highlight CALF's capacity to outperform traditional methods in terms of reactive power calculation precision. While its precision advantage over NR might lessen with larger grid sizes, CALF continues to exhibit superior performance compared to the GS method. These findings reinforce the suitability of the CALF method for a wide range of grid sizes, affirming its potential as a robust solution for reactive power analysis.

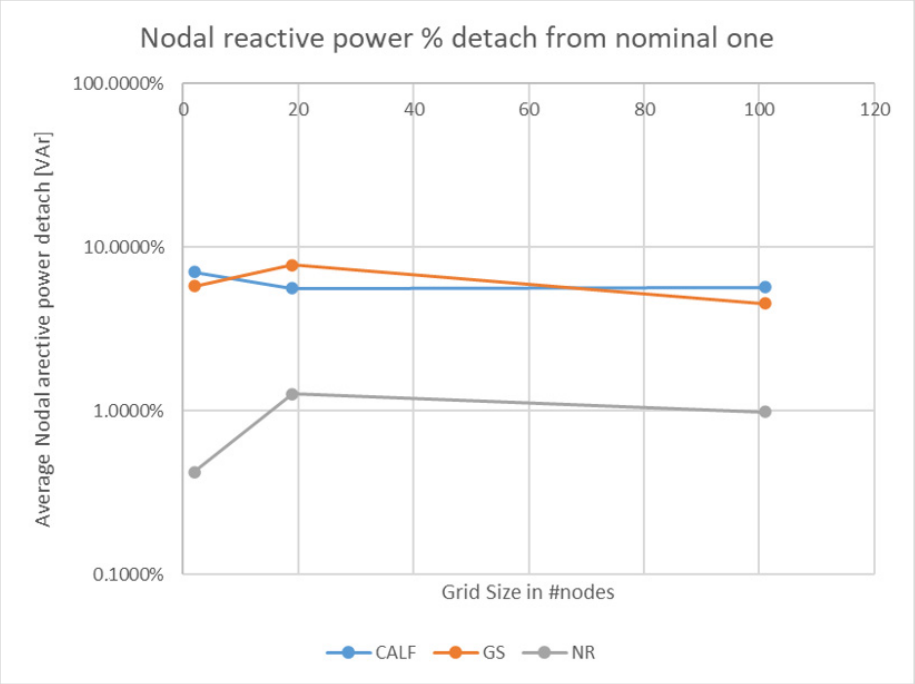

Figure 15. Representation nodal reactive power % detachment from slack bus supplied reactive power.

4.5. LF with Changing Initial Nodal Voltage Flat Start

In this section, the robustness testing of the methods when compared with varying flat start conditions was observed. The objective was to discern how the execution time is affected when the initial guess value for nodal voltages deviates from the nominal value. This assessment aims to gauge the methods' responsiveness to alterations in initial conditions. To simulate this scenario, a range of initial guess values was obtained by detaching from the nominal voltage. The detachment levels encompass +10%, 1%, 0.1%, 0.01%, and 0%. Across different grid sizes (2, 19, and 101 nodes), the execution time results for the CALF, GS, and NR methods are presented in Tables 14–16. These tables distinctly illustrate how the execution time is influenced by varying detachment levels from nominal voltage as initial guess values (flat start) (Figure 16).

Table 14. Execution time vs. grid size for CALF, considering a % detachment from nominal voltage as flat start.

Node Number	10% Detachment from Nominal Voltage Flat Start	1%	0.1%	0.01%	0%
2	0.9968	0.153	0.5189	1.0036	0.9978
19	1.9963	2.9907	5.9842	12.989	10.44368744
101	20.64484	33.8026	15.9574	21.294	17.95220375

Table 15. Execution time vs. grid size for GS, considering a % detachment from nominal voltage as flat start.

Node Number	10% Detachment from Nominal Voltage Flat Start	1%	0.1%	0.01%	0%
2	0.9929	1.0037	0.9977	1.0005	0.9967
19	0.9978	3.9902	1.9935	10.97	9.739739275
101	53.9628	70.9717	63.9622	45.9558	39.54172134

Table 16. Execution time vs. grid size for NR, considering a % detachment from nominal voltage as flat start.

Node Number	10% Detachment from Nominal Voltage Flat Start	1%	0.1%	0.01%	0%
2	1.9954	0.9976	1.9847	2.987	3.7756
19	31.9124	50.8657	40.8885	21.8795	19.93894577
101	92.25319	108.41114	65.32519	32.62957	20.02763748

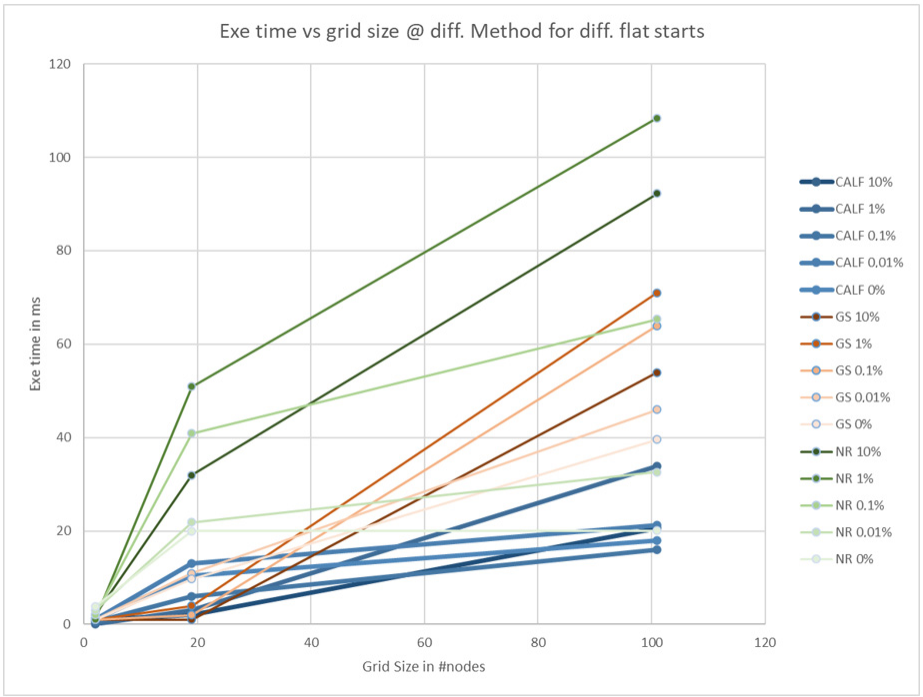

Figure 16. Execution time vs. grid size for different methods and detachment from nominal voltage as flat start.

The insights derived from the results are as follows: CALF exhibits higher robustness compared to NR and GS methods, showcasing its ability to maintain a consistent execution time across detachment levels from the nominal voltage. As the detachment percentage decreases, CALF's execution time remains relatively stable. In contrast, NR and GS methods display a significant increase in execution time as the detachment level decreases. This differential behavior underscores the design effectiveness of CALF, as it ensures efficient and steady convergence even in scenarios where initial guess values deviate from the nominal voltage.

4.6. Advantages and Limitations of CALF Method

The realm of load flow analysis involves a diverse spectrum of methodologies, each carrying its own set of advantages and limitations. To better understand the implications of the CALF method, we systematically conducted and reviewed an array of precision, robustness, and performance tests. In doing so, the aim was to evaluate the efficacy of CALF in comparison to two widely employed techniques: the Newton–Raphson (NR) and Gauss–Seidel (GS) methods. The synthesis of these assessments allows us to address the reviewer's query regarding the inherent strengths and weaknesses of LF methodologies.

Advantages of CALF:

- Precision and accuracy: The precision tests unveiled that the CALF method consistently delivered highly accurate nodal voltage and active/reactive power results, often surpassing the GS method and, in specific scenarios, rivalling the precision of the NR method.
- Robustness: In the context of robustness, CALF exhibited a notable advantage over NR and GS. Its execution time remained relatively constant even with deviations from nominal voltage as initial guesses, signifying its resilience in converging swiftly across different starting conditions.
- Efficiency: CALF demonstrated efficiency by consistently outperforming NR in terms of execution time. Its computational speed was particularly evident for larger grids, where CALF's execution time was significantly shorter than both NR and GS.
- Simplicity and elegance: Unlike the intricate iterative processes of NR and GS, CALF's linear solution approach showcases a streamlined and elegant design. This simplicity potentially leads to fewer convergence issues.

Limitations of CALF:

- Precision in larger grids: While CALF demonstrated exceptional precision for smaller to medium-sized grids, its performance slightly diminished with larger grid sizes. In these cases, the precision advantage over NR became less pronounced.
- Combined method performance: Our combined methods test indicated that the execution time of the CALF-NR and CALF-GS combined methods was less efficient than CALF alone. While CALF still outperformed NR and GS, the combination resulted in a slight compromise in performance.
- Initial guess sensitivity: While CALF's robustness was evident, it is important to note that like all iterative methods, it can be sensitive to initial guess values. Although this sensitivity was mitigated by CALF's robustness design, careful initialization remains relevant.

In conclusion, the CALF method offers a distinct set of advantages, including exceptional precision, robustness, efficiency, and elegance. While it excels in various aspects, its performance characteristics vary with grid size and combined method execution. By conducting meticulous assessments and comparing CALF with established methodologies, we strive to provide a comprehensive understanding of its strengths and limitations, thereby contributing to bridging the existing gap in our research.

5. Conclusions

In summary, this paper introduces the CALF method as a novel approach for solving load flow problems in power systems. The CALF method, designed as a linear and iterative technique, offers a promising alternative to traditional methods like the Newton–Raphson (NR) and Gauss–Seidel (GS) approaches. By harnessing its inherent advantages, CALF significantly enhances the load flow analysis process. The extensive evaluation conducted in this study sheds light on various facets of CALF's performance.

The comprehensive testing and analysis underscore the robustness and efficiency of the CALF method. In particular, its ability to achieve superior accuracy while exhibiting commendable execution speed, especially for grid sizes typical of medium and low-voltage networks in Italy, sets it apart from conventional methods. The tests for nodal voltage, active power, and reactive power detachment reveal CALF's precision, further solidifying its position as a valuable tool for load flow analysis.

Moreover, the CALF method's versatility extends to robustness, as demonstrated through its resistance to variations in initial guess values for nodal voltages. The consistent execution time across varying detachment percentages from nominal voltage underscores CALF's reliability and efficiency, particularly in real-world scenarios where initial estimates can vary.

Addressing the need for CALF's applicability, we emphasize that its enhanced performance is specific to certain conditions, particularly within Italian electrical networks characterized by medium- and low-voltage grids. By highlighting CALF's alignment with these scenarios, we ensure a transparent understanding of its value proposition and the contexts in which it excels.

While we acknowledge that the CALF method is not without its limitations, we appreciate the importance of future research in addressing these constraints, especially to extend the method for bigger grids typically for MV and HV lines. Our commitment to ongoing exploration is reflected in CALF's potential application for calculating hosting and load capacity in power systems—a domain vital for energy utilities' effective grid management. The simplicity and ease of CALF's implementation, facilitating low-cost cloud deployment, adds another layer of value to its practicality.

In conclusion, the CALF method offers a strategic leap forward in the field of load flow analysis, transcending traditional methods with its speed, accuracy, and adaptability to specific network scenarios. We enhance the robustness of our conclusions by acknowledging limitations and charting future research avenues, striving to present CALF not only as a solution but as a catalyst for innovative advancements in power systems engineering.

Author Contributions: Conceptualization, B.-G.R. and A.L.; Validation, M.Q.; Supervision, F.R.-F. All authors have read and agreed to the published version of the manuscript.

Funding: This research received no external funding.

Informed Consent Statement: Not applicable.

Data Availability Statement: No applicable.

Conflicts of Interest: The authors declare no conflict of interest.

References

1. Milano, F. Analogy and Convergence of Levenberg's and Lyapunov-Based Methods for Power Flow Analysis. *IEEE Trans. Power Syst.* **2016**, *31*, 1663–1664. [CrossRef]
2. Hamedi, M.; Shayeghi, H.; Seyedshenava, S.; Safari, A.; Younesi, A.; Bizon, N.; Iana, V.-G. Developing an Integration of Smart-Inverter-Based Hosting-Capacity Enhancement in Dynamic Expansion Planning of PV-Penetrated LV Distribution Networks. *Sustainability* **2023**, *15*, 11183. [CrossRef]
3. Lazzeroni, P.; Mariuzzo, I.; Quercio, M.; Repetto, M. Economic, Energy, and Environmental Analysis of PV with Battery Storage for Italian Households. *Electronics* **2021**, *10*, 1919. [CrossRef]
4. Montoya, F.G.; Baños Navarro, R. *Optimization Methods Applied to Power Systems II*; MDPI—Multidisciplinary Digital Publishing Institute: Basel, Switzerland, 2021.

5. El-Hawary, M.E. (Ed.) *Advances in Electric Power and Energy Systems: Load and Price Forecasting*; Wiley: Hoboken, NJ, USA, 2017.
6. Lin, J.; Li, V.O.K.; Leung, K.-C.; Lam, A.Y.S. Optimal Power Flow with Power Flow Routers. *IEEE Trans. Power Syst.* **2017**, *32*, 531–543. [CrossRef]
7. Low, S.H. Convex Relaxation of Optimal Power Flow—Part I: Formulations and Equivalence. *IEEE Trans. Control Netw. Syst.* **2014**, *1*, 15–27. [CrossRef]
8. Faba, A.; Gaiotto, S.; Lozito, G.M. A novel technique for online monitoring of photovoltaic devices degradation. *Sol. Energy* **2017**, *158*, 520–527. [CrossRef]
9. Miah, M.S.; Hossain Lipu, M.S.; Meraj, S.T.; Hasan, K.; Ansari, S.; Jamal, T.; Masrur, H.; Elavarasan, R.M.; Hussain, A. Optimized Energy Management Schemes for Electric Vehicle Applications: A Bibliometric Analysis towards Future Trends. *Sustainability* **2021**, *13*, 12800. [CrossRef]
10. Sun, B.; Jing, R.; Zeng, Y.; Li, Y.; Chen, J.; Liang, G. Distributed Optimal Dispatching Method for Smart Distribution Network Considering Effective Interaction of Source-Network-Load-Storage Flexible Resources. *Energy Rep.* **2023**, *9*, 148–162. [CrossRef]
11. Mastoi, M.S.; Zhuang, S.; Munir, H.M.; Haris, M.; Hassan, M.; Alqarni, M.; Alamri, B. A Study of Charging-Dispatch Strategies and Vehicle-to-Grid Technologies for Electric Vehicles in Distribution Networks. *Energy Rep.* **2023**, *9*, 1777–1806. [CrossRef]
12. Corti, F.; Reatti, A.; Pierini, M.; Barbieri, R.; Berzi, L.; Nepote, A.; De La Pierre, P. A Low-Cost Secondary-Side Controlled Electric Vehicle Wireless Charging System using a Full-Active Rectifier. In Proceedings of the 2018 International Conference of Electrical and Electronic Technologies for Automotive, Milan, Italy, 9–11 July 2018; pp. 1–6.
13. Pandey, A.; Jereminov, M.; Wagner, M.R.; Bromberg, D.M.; Hug, G.; Pileggi, L. Robust Power Flow and Three-Phase Power Flow Analyses. *IEEE Trans. Power Syst.* **2019**, *34*, 616–626. [CrossRef]
14. Simpson-Porco, J.W. A Theory of Solvability for Lossless Power Flow Equations—Part I: Fixed-Point Power Flow. *IEEE Trans. Control Netw. Syst.* **2018**, *5*, 1361–1372. [CrossRef]
15. Corti, F.; Laudani, A.; Lozito, G.M.; Palermo, M.; Quercio, M.; Pattini, F.; Rampino, S. Dynamic Analysis of a Supercapacitor DC-Link in Photovoltaic Conversion Applications. *Energies* **2023**, *16*, 5864. [CrossRef]
16. Kamel, S.; Jurado, F.; Chen, Z.; Abdel-Akher, M.; Ebeed, M. Developed Generalised Unified Power Flow Controller Model in the Newton–Raphson Power-Flow Analysis Using Combined Mismatches Method. *IET Gener. Transm. Distrib.* **2016**, *10*, 2177–2184. [CrossRef]
17. Talluri, G.; Lozito, G.M.; Grasso, F.; Iturrino Garcia, C.; Luchetta, A. Optimal battery energy storage system scheduling within renewable energy communities. *Energies* **2021**, *14*, 8480. [CrossRef]
18. Pugi, L.; Reatti, A.; Corti, F. Application of Wireless Power Transfer to Railway Parking Functionality: Preliminary Design Considerations with Series-Series and LCC Topologies. *J. Adv. Transp.* **2018**, *2018*, 8103140. [CrossRef]
19. Luca, P.; Reatti, A.; Corti, F.; Mastromauro, R.A. Inductive power transfer: Through a bondgraph analogy, an innovative modal approach. In Proceedings of the 2017 IEEE International Conference on Environment and Electrical Engineering and 2017 IEEE Industrial and Commercial Power Systems Europe (EEEIC/I&CPS Europe), Milan, Italy, 6–9 June 2017; pp. 1–6.